NASA/TM-2004-213499

A Hierarchical Approach to Fracture Mechanics

Erik Saether
Langley Research Center, Hampton, Virginia

Shlomo Ta'asan
Carnegie Mellon University, Pittsburgh, Pennsylvania

November 2004

The NASA STI Program Office . . . in Profile

Since its founding, NASA has been dedicated to the advancement of aeronautics and space science. The NASA Scientific and Technical Information (STI) Program Office plays a key part in helping NASA maintain this important role.

The NASA STI Program Office is operated by Langley Research Center, the lead center for NASA's scientific and technical information. The NASA STI Program Office provides access to the NASA STI Database, the largest collection of aeronautical and space science STI in the world. The Program Office is also NASA's institutional mechanism for disseminating the results of its research and development activities. These results are published by NASA in the NASA STI Report Series, which includes the following report types:

- TECHNICAL PUBLICATION. Reports of completed research or a major significant phase of research that present the results of NASA programs and include extensive data or theoretical analysis. Includes compilations of significant scientific and technical data and information deemed to be of continuing reference value. NASA counterpart of peer-reviewed formal professional papers, but having less stringent limitations on manuscript length and extent of graphic presentations.

- TECHNICAL MEMORANDUM. Scientific and technical findings that are preliminary or of specialized interest, e.g., quick release reports, working papers, and bibliographies that contain minimal annotation. Does not contain extensive analysis.

- CONTRACTOR REPORT. Scientific and technical findings by NASA-sponsored contractors and grantees.

- CONFERENCE PUBLICATION. Collected papers from scientific and technical conferences, symposia, seminars, or other meetings sponsored or co-sponsored by NASA.

- SPECIAL PUBLICATION. Scientific, technical, or historical information from NASA programs, projects, and missions, often concerned with subjects having substantial public interest.

- TECHNICAL TRANSLATION. English-language translations of foreign scientific and technical material pertinent to NASA's mission.

Specialized services that complement the STI Program Office's diverse offerings include creating custom thesauri, building customized databases, organizing and publishing research results ... even providing videos.

For more information about the NASA STI Program Office, see the following:

- Access the NASA STI Program Home Page at ***http://www.sti.nasa.gov***

- E-mail your question via the Internet to help@sti.nasa.gov

- Fax your question to the NASA STI Help Desk at (301) 621-0134

- Phone the NASA STI Help Desk at (301) 621-0390

- Write to:
  NASA STI Help Desk
  NASA Center for AeroSpace Information
  7121 Standard Drive
  Hanover, MD 21076-1320

NASA/TM-2004-213499

A Hierarchical Approach to Fracture Mechanics

Erik Saether
Langley Research Center, Hampton, Virginia

Shlomo Ta'asan
Carnegie Mellon University, Pittsburgh, Pennsylvania

National Aeronautics and
Space Administration

Langley Research Center
Hampton, Virginia 23681-2199

November 2004

Available from:

NASA Center for AeroSpace Information (CASI)
7121 Standard Drive
Hanover, MD 21076-1320
(301) 621-0390

National Technical Information Service (NTIS)
5285 Port Royal Road
Springfield, VA 22161-2171
(703) 605-6000

Abstract

Recent research conducted under NASA LaRC's Creativity and Innovation Program has led to the development of an initial approach for a hierarchical fracture mechanics. This methodology unites failure mechanisms occurring at different length scales and provides a framework for a physics-based theory of fracture. At the nanoscale, parametric molecular dynamic simulations are used to compute the energy associated with atomic level failure mechanisms. This information is used in a mesoscale percolation model of defect coalescence to obtain statistics of fracture paths and energies through Monte Carlo simulations. The mathematical structure of predicted crack paths is described using concepts of fractal geometry. The non-integer fractal dimension relates geometric and energy measures between meso- and macroscales. For illustration, a fractal-based continuum strain energy release rate is derived for inter- and transgranular fracture in polycrystalline metals.

Keywords: fracture mechanics, strain energy release rate, fractal geometry

1.0 Introduction

Classical Fracture Mechanics is based on a continuum description of material domains and fracture behavior described in terms of empirical parameters such as critical strain energy release (G_C), resistance curves (J-R), and crack tip opening angles (CTOA), etc. Advances in computer systems are making it increasingly possible to study the behavior of materials using computational methods that simulate the interaction and evolution of defects in atomic ensembles under applied loads. These analyses simulate fundamental material processes using *first principles* in physics and provide an ultimate understanding of deformation and fracture at the atomic level. A hierarchical description of fracture can be modeled using fractal concepts that naturally permit transitioning between length scales. This modeling of fracture is based on the observation that crack paths and fracture surfaces exhibit fractal characteristics of self-similarity over a range of length scales. Geometric self-similarity asserts that topologically congruent or equivalent features exist at each dimensional scale and implies that the atomic scale may be directly related to the macroscopic continuum scale through a fractal description. The transformation of information of the underlying physics of crack growth across length scales has the potential of dramatically reducing empiricism in the description of fracture and may be considered a new approach to fracture mechanics.

The ultimate goal of the present research is to develop a unified framework in which classical continuum fracture parameters are replaced with fractal definitions to provide scale-independent ‘true’ material constants. For this initial effort, this framework seeks to combine different computational methods and geometrical descriptions across dimensional scales to incorporate atomistic failure mechanisms within the definition of macroscopic fracture measures. A fractal description of geometry yields a formalism in which the actual length of a crack and the true area of fracture surfaces can be represented. Various features of crack propagation such as crack path length, branching and consolidation may be simulated using a variety of fractal methods. The energetics of

nanoscale fracture mechanisms can be calculated using molecular dynamic (MD) simulation methods and can be scaled in an implicitly bottom-up approach within a hierarchical fracture mechanics paradigm.

This report is divided into two parts. The first part details issues related to the theoretical formulation of a new approach to fracture mechanics wherein basic definitions, mathematical modeling approaches, and material systems are discussed. A fractal-based continuum strain energy release rate is defined. The second part describes a practical implementation of the developed theoretical formulation in which damage mechanisms are related over length scales. Illustrative simulation results are presented and future research directions are discussed in the conclusion.

2.0 Theoretical Development

The following subsections discuss fracture mechanics issues related to the hierarchical analysis of polycrystalline metals. These include a description of a hierarchical fracture analysis, brittle and ductile material fracture behavior, and the energetics of fracture. An introduction to fractal geometry is detailed which provides a scale-independent approach for defining a strain energy release rate based on atomistic simulation of fundamental fracture mechanisms that can be converted to a macroscopic definition.

2.1 Overview of a Hierarchical Fracture Mechanics Approach

The overall theoretical framework consists of developing a hierarchical methodology to simulate and link fracture phenomena exhibited at different characteristic length scales. At the nanoscale (10^{-9}m - 10^{-7}m), computations involve atomistic simulation of voids, pores, intergranular and transgranular, and dislocation formation, while accounting for grain size, orientation and boundary characteristics. For transitioning to the mesoscale (10^{-7}m - 10^{-5}m), a continuum model of polycrystalline grain configurations is developed to simulate realistic cracks from which fracture statistics are generated. Material-specific grain configurations are generated through Monte Carlo simulations and the response of the model under applied loads is calculated using a discrete finite element procedure. Material properties used in this model are obtained from parametric studies of grain deformation and grain boundary response using atomistic analysis. Three important calculations are performed using the mesoscale continuum model: (i) Failure progression caused by the development and coalescence of defects; (ii) the computation of statistical characteristics of fracture such as number of crack segments, orientation of crack paths, and lengths; and (iii) the development of probability density functions for grain boundary misorientation angles and grain boundary orientation with respect to far-field applied loads. The fractal properties of cracks are modeled by introducing spatial distribution functions that represent the geometrical aspects characterizing fracture surfaces and allow an accurate integration of energies along these rough surfaces. The separation energy density is integrated using the statistical characterizations of the mesostructure and the spatial distribution functions. The fractal dimension of the fracture surface provides a scale factor resulting in a total energy measure valid at the macroscale (10^{-3}m – 10^{0}m).

2.2 Hierarchical Fracture Processes across Length Scales

Classical theory defines three fundamental modes of fracture based on macroscopic relative displacement profiles which are depicted in Figure 1. However, small-scale failure mechanisms operating within the process zone around the crack tip generate complex local deformation fields that preclude simple descriptions. While providing a basis for categorizing continuum fracture, each macroscopic mode of fracture will typically involve all three relative deformation modes locally within the process zone at the microscale. These deformation modes consist of a hierarchy of self-similar fracture mechanisms occurring at different length scales contributing to the evolving deformation state. Thus, the fundamental notion of distinct modes used in classical fracture mechanics becomes ill-defined when smaller-scale processes are accounted in a hierarchical analysis. The lowermost length scale is on the order of nanometers and defines the realm of atomistic interactions at which all material failure phenomena originates. This hierarchy of length scales for a polycrystalline metal is depicted in Figure 2.

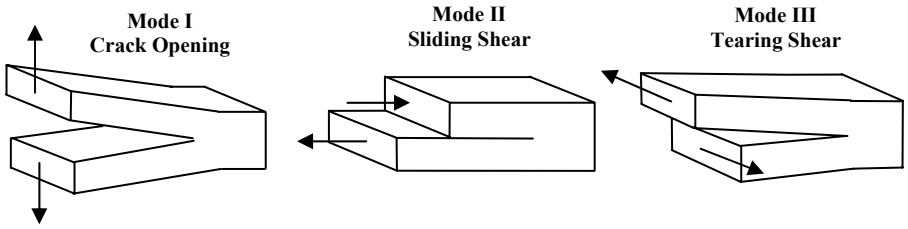

Figure 1. Fundamental fracture modes in solids.

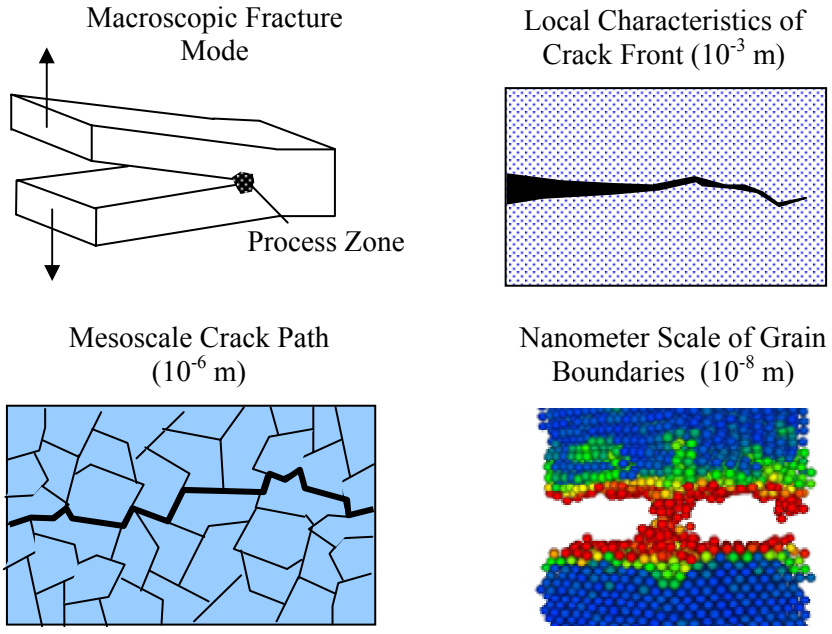

Figure 2. Fracture processes at different length scales.

Experimentally determined fracture parameters measure a homogenization of many failure mechanisms operating at different length scales. These fracture mechanisms include nanoscopic dislocation formation and interaction, voids, pores, precipitation aggregates, mesoscale intergranular and transgranular cleavage, and macroscopic fracture surface development and propagation.

The granular structure of a metallic material is responsible for many of its fundamental properties. As materials undergo work, initial defects enlarge and new defects are created. Of particular interest are nanoscopic failure processes that coalesce into microcracks that develop further into large-scale cracks causing loss of structural integrity or catastrophic material failure. Some of these cracks may consist exclusively of intergranular decohesion along grain boundaries, while others may include predominantly transgranular fracture though the grains. For brittle materials, the energy that it takes to break a material typically depends on the total extent of intergranular fracture surface that is formed.

The hallmark of current fracture mechanics has been the integration of experimental measurements of fracture, such as toughness and fatigue crack growth rates, within a theoretical framework [1]. This framework, however, typically assumes a phenomenological approach that is empirical in nature. In addition, the restriction of using integer Euclidean dimensions for defining length and area measures of fracture geometry results in assumed geometric descriptions that possess little relation to actual crack paths and the geometric texture of fracture surfaces. Atomistic simulation of fundamental failure processes combined with fractal descriptions of fracture geometry allows the theory of fracture to be extended by incorporating mechanisms that operate at different length scales [2, 3].

2.3 Brittle versus Ductile Failure Processes

The dominant energy consumption in the fracture of brittle materials is associated with the creation of fracture surfaces within the solid [4]. In polycrystalline metals, brittle failure involves primarily the separation energy of grain boundary interfaces with little contribution from work due to plastic deformation within grains. In ductile materials, however, the energy associated with plastic deformation becomes predominant. For both types of materials it may be assumed that nanoscopic defects are scattered randomly throughout the material region and undergo coalescence. Within this field of defects, the local intensification of nanostresses enhances the coalescence of nanodefects, ultimately converging into a sparse distribution of larger cracks that tend to consume a majority of the input energy. The extent of these cracks fall into the ‘small-crack’ regime wherein the crack length, l_c, is bounded by $100\,\mu\text{m} \le l_c \le 1\,\text{mm}$. At this length scale, the crack is influenced by a surrounding heterogeneous microstructural state but can be approximated by continuum modeling approaches. As ‘small-cracks’ coalesce, dominant cracks develop in ductile materials and the local stress intensity leads to the development of a large surrounding plastic region. As local yield stresses are exceeded at the atomic level, initial ‘easy glide’ dislocations develop on various available glide planes. With increasing strain, the interaction of slip systems on different glide planes becomes increasingly

complex and dictates the nature of overall plastic deformation within grains. The presence of various forms of locking in interacting dislocation systems typically harden a material such that further deformation cannot be accommodated through the movement of dislocations, thus leading to local failure. These phenomena need to be characterized statistically and incorporated into the current model.

The overall crack path will be determined by the pattern of propagation along minimum energy paths in the process zone which typically exhibits fractal characteristics. Various models of grain deformation such as strain gradient plasticity [5] may prove ideally suited for simulating ductile material response at mesoscopic length scales. The current hierarchical model is limited to brittle failure but incorporates a mesoscale continuum model that can be enhanced to include plasticity. This extension of the present analysis to model ductile material behavior is a topic for future research.

2.4 Mathematics of Fractal Geometry

Fractal geometry was originally developed by Mandelbrot [6] and has matured into a broad area of mathematics [7, 8]. These geometric concepts provide a rigorous representation of irregular yet structured patterns of natural phenomena exhibited over a sequence of length scales. Fractal geometries are generated iteratively and possess an extent that is dependent on the length scale at which segments are measured. For applications to fracture mechanics, the fractal properties of self-similarity, self-affinity, and multifractality are of particular utility in rigorously defining the texture of crack geometry that exist at different dimensional scales. Figure 3 shows examples of the iterative generation of fractals that provides an intuitive understanding to the concept of self-similarity. The construction consists of replacing a repeating unit of the geometry with a scaled representation of the overall pattern following a scheme known as a generator. For the Box Fractal, each solid square is replaced by a configuration of five smaller squares with missing spaces as shown. The Seirpinski Sieve Fractal is formed by recursively replacing each equilateral triangle with three smaller triangles with a missing triangle in the center.

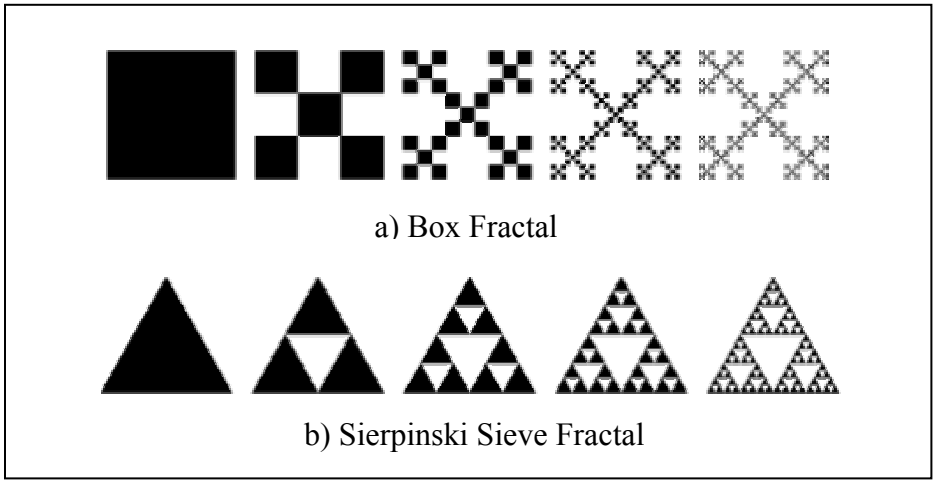

Figure 3. Examples of geometric transformations yielding fractals.
(http://mathworld.wolfram.com/Fractal.html)

Self-affinity is related to self-similarity, differing only in a greater freedom by scaling the geometry unequally at each iteration of the generator in creating the fractal geometry. Multifractility refers to another increase in modeling freedom by allowing different generators to operate at different dimensional length scales.

The operations used to generate the fractals in Figure 3 can be expressed rigorously in terms of linear transformations that define how one characteristic shape or generator can be mapped between geometric iterations. In two-dimensions, the linear transformation corresponding to the generation of a self-similar fractal object between the i^{th} and $(i+1)^{st}$ iteration may be described as

$$\begin{Bmatrix} x_1^{(i+1)} \\ x_2^{(i+1)} \end{Bmatrix} = \begin{bmatrix} \lambda & 0 \\ 0 & \lambda \end{bmatrix} \begin{Bmatrix} x_1^{(i)} \\ x_2^{(i)} \end{Bmatrix} + \begin{Bmatrix} \beta \\ \beta \end{Bmatrix} \tag{1}$$

where λ and β are stretching and translation parameters, respectively. This transformation generates a geometrically isotropic fractal where features are identical in both the x_1 and x_2 coordinates. A related construction yields a fractal with the property of self-affinity. This transformation is given by

$$\begin{Bmatrix} x_1^{(i+1)} \\ x_2^{(i+1)} \end{Bmatrix} = \begin{bmatrix} \lambda_{11} & \lambda_{12} \\ \lambda_{21} & \lambda_{22} \end{bmatrix} \begin{Bmatrix} x_1^{(i)} \\ x_2^{(i)} \end{Bmatrix} + \begin{Bmatrix} \beta_1 \\ \beta_2 \end{Bmatrix} \tag{2}$$

which contains different scale factors for x_1 and x_2, leading to a general directional dependence or anisotropy of the fractal object. A more general geometry exhibiting multifractility can be given as a sequence of linear transformations such as Equations (1) and (2) with mapping parameters that change with the iteration index i.

Figure 4 shows two variations of a self-similar fractal known as the Koch Curve [8]. This curve has a direct application to modeling two-dimensional crack paths and shows how the geometry can be modified through the construction rules. The construction begins with an initiator of length L_o shown at the top of Figure 4 which is then recursively modified by replacing each straight segment by the pattern of the generator. For the Basic Koch Curve, each iteration, n, replaces a straight segment by four smaller segments. Thus, at the n^{th} iteration, the total number of straight segments, N_n, is equal to 4^n. Because the distance between the endpoints of the initiator is kept constant, the new segment lengths, ε_n, are equal to $L_o/3^n$. For the Modified Koch Curve, the generator is more complex such that at each iteration, N_n is equal to 6, and ε_n is equal to $L_o/[2+4Sin(\alpha/2)]$. As shown graphically in the figure, modifications to the generator have a profound effect on the resulting fractal. While the Basic Koch Curve clearly shows self-similar features with increasing refinement, the self-similarity of the Modified Koch Curve is only discerned under scrutiny and the resulting geometry of the curve begins to display a distinctly 'crack-like' appearance.

The product of the number of segments and the segment length yields a fundamental relationship for self-similar fractals that can be expressed as:

$$N_n(\varepsilon) \times \varepsilon_n^D = \text{const.} \tag{3}$$

where D is a fractional exponent that is a fundamental characteristic of the fractal. Arbitrary values of D cause the product to converge to zero or infinity; the value that yields a constant product uniquely determines this exponent and is referred to as the Hausdorff dimension of the fractal [7].

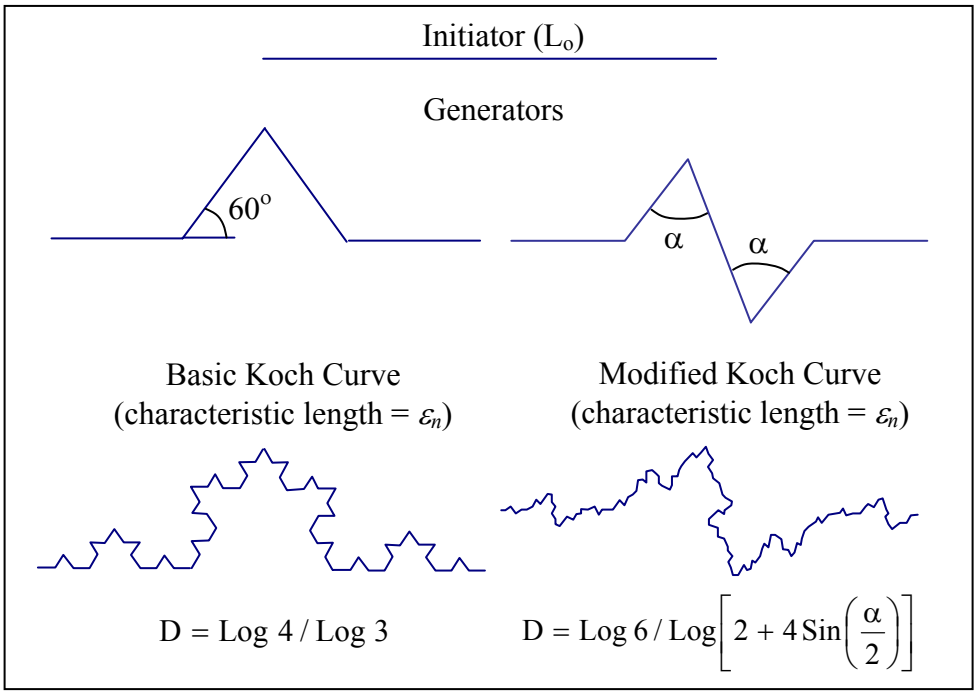

Figure 4. Self-similar Koch curves.

A manipulation of Equation (3) yields an expression for the total length, L_n, at the n^{th} iteration of the fractal given by

$$L_n = L_o^D \, \varepsilon_n^{1-D} \tag{4}$$

A distinction can be made between mathematical and physical fractals. In a mathematical fractal, the iterations continue indefinitely such that the resulting geometry is nonrectifiable (indeterminate length) and nondifferentiable at every point. In application to fracture mechanics, however, physical fractals are defined using a minimum bounding length scale which eliminates the infinite descent of geometric features along the fractal curve.

The maximum feature length is the macroscopic scale where the fracture surface is projected onto a flat surface, and the smallest scale, ε, corresponds to the smallest physical crack feature such as a characteristic grain boundary length or an interatomic spacing. The disparity between Euclidian measures of crack extension and fractal

measures can be significant. For example, if we look at the length magnification of the modified Koch curve, taking $\alpha = 30^o$ and a characteristic length of 0.0358 times the length of the initiator (taken as unity here), one obtains a fractal dimension of 1.6138 and, from Equation (4), a length magnification of 7.733. Thus, utilizing a more realistic geometry for surface texture, the total area of fracture surface creation is highly increased compared to simple smooth crack geometry assumptions.

To determine fractal dimensions of fracture surfaces from experimental data, such as fractographic imaging, various methods may be applied. These methods include slit island analysis (SIA) [9], fracture profile analysis (FPA) based on a Fourier analysis of the fracture surface [10,11], vertical section method (VSM), and box counting or variation method [12]. Experimental errors in determining fractal dimensions can be significant. However, in the present analysis, fractal dimensions are determined using an intermediate mesoscale model. This continuum model incorporates the basic physics of grain formation and stability and defect distribution from which statistically valid fractal dimensions can be determined from a Monte Carlo simulation.

In the present analysis, the Hausdorff dimension *D* is obtained using a variation of the box counting method. This approach is based on the measurement approach of counting the number of boxes, circles or spheres required to 'cover' a fractal object at various length scales. This is obtained from Equation (3) by setting the arbitrary constant to unity such that:

$$N_i = \varepsilon_i^{-D} \quad \text{or} \quad D = -\,\mathrm{Log}(N_i)/\mathrm{Log}(\varepsilon_i) \tag{5}$$

where ε_i is a characteristic size of the covers and N_i is the number of covers that are intersected by the fractal object. The covering procedure is depicted in Figure 5 where $R_i = \varepsilon_i/2$, and the fractal dimension is determined from Equation (5) by computing the slope of a log-log plot of measurements shown in Figure 6.

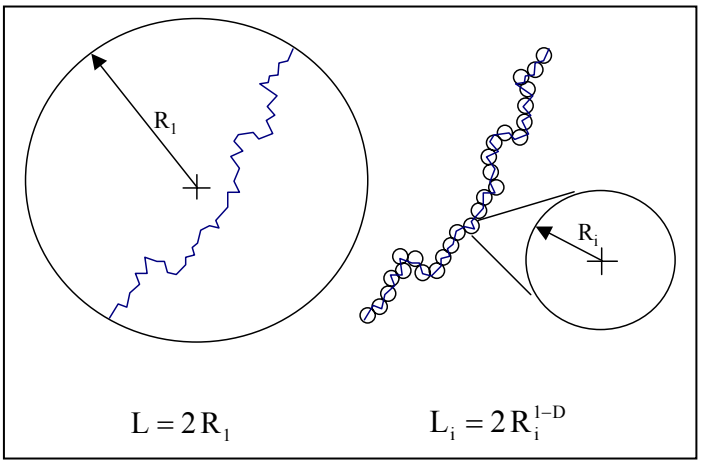

Figure 5. Covering method for determining fractal dimension.

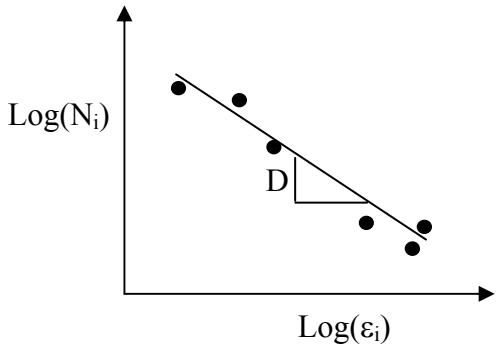

Figure 6. Linear regression fit to determine fractal dimension D.

2.5 Fractal Characteristics of Fracture

A fundamental observation regarding material fracture is that the geometry of crack paths, crack fronts, and surface texture demonstrate fractal characteristics [13,14]. Thus, fracture measurements do not generally possess a linear scaling behavior and, instead, exhibit a size dependence [15]. This means that if an experiment is performed for a specimen of 1 cm in length, the result may not apply to a specimen of 1 micron in length. In general, fracture can exhibit ranges in which the fractal dimension changes due to different scale-dependent fracture mechanisms which give rise to multifractal and multi-affine models. It has also been observed that certain materials possess regions at higher length scales at which the fractality disappears and the fractional dimension is replaced by an integer Euclidean measure thus eliminating size dependence.

In practice, naturally occurring fractal objects are typically irregular to various degrees but may still be characterized as self-similar in a statistical sense. Self-similarity is required for a Hausdorff dimension to be uniquely defined, however, numerous other fractal constructs exist which may be used in the context of more involved fractal constructs such as self-affinity and multifractals. These representations involve transformations that can be generally anisotropic with fractal dimensions that can vary between levels of fractal generation. Examples of fracture processes exhibiting fractal characteristics are presented in Figure 7.

Fractal descriptions can be used for many of the processes of failure at the mesoscale level. Crack branching, front development, surface generation, void coalescence, dislocation interactions, and the irreversible deformation of material domains can all be cast as fractal processes and quantified with suitable fractal representations.

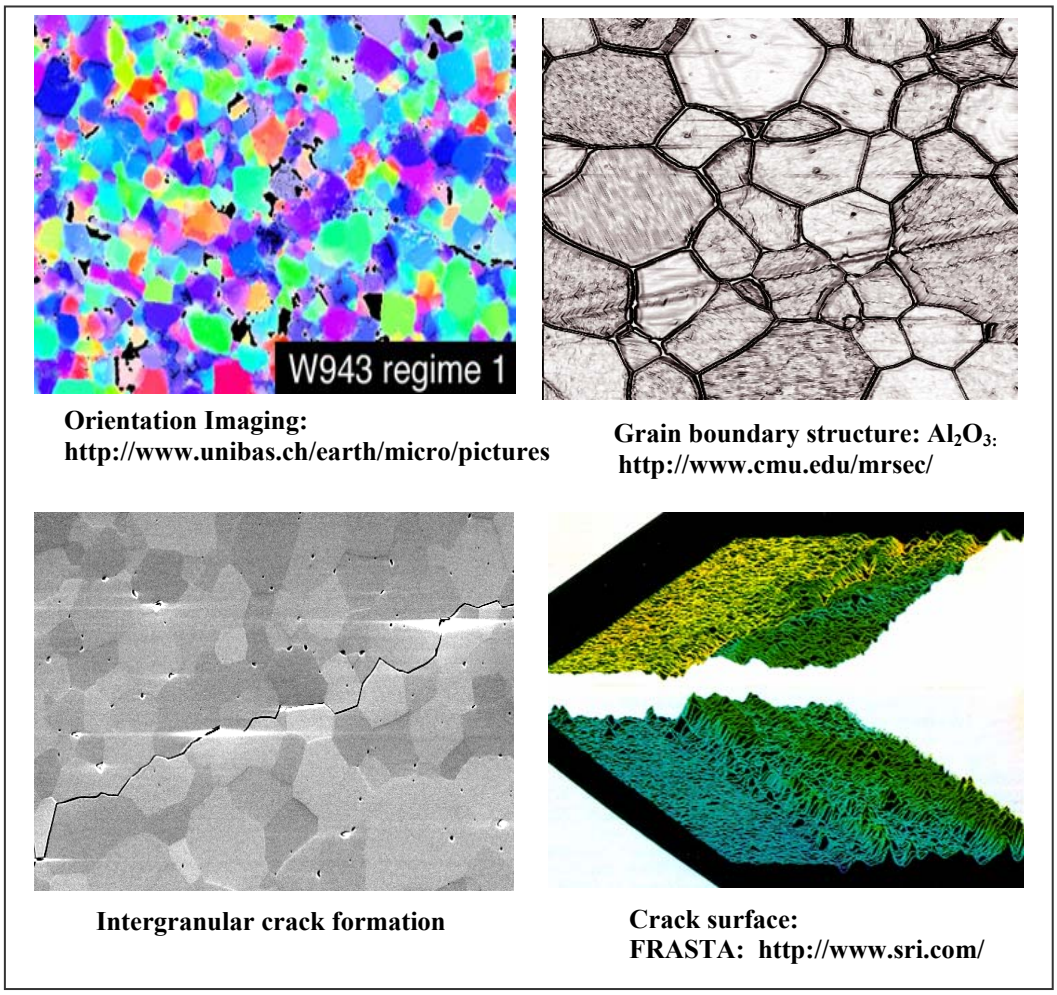

Figure 7: Geometry of grain boundaries and fracture [16].

In classical fracture mechanics, simplified formulae for strain energy release rates utilize a fracture surface area based on integer dimensions. This assumes that the fracture surface is smooth, and its area is simply a product of a length and width. Real fracture surfaces, however, are generally rough or textured, and a Euclidean measure of surface area leads to an incorrect estimate of quantities such as critical strain energy release rate (fracture toughness) based on the creation of new surface area. The main problem is that classical descriptions of material geometry and failure processes are based entirely on integer or Euclidean dimensions for length and surface metrics to define fracture parameters. This has contributed to the common observation that theoretical predictions of critical strain energy release rates are orders of magnitude below experimentally measured values. The underlying geometry of fracture is, however, generally non-Euclidean and is more accurately described by self-similar or self-affine fractal geometric measures possessing non-integer fractal dimensions. Thus, classical measures fail to

capture the microstructure of a fracture surface and the effective area relevant to energy calculations.

Previous investigations have been published in which fractal geometry constructs have been directly incorporated into classical continuum definitions of fracture mechanics, and has led to redefinitions of stress intensities and the introduction of 'new' fracture modes [17-19]. For example, incorporating fractal geometry into the expression for the classical crack tip stress field associated with Mode I fracture yields

$$\sigma_{ij}(r,\theta) = K_1 r^{\frac{D-2}{2}} \varphi(\theta) \tag{6}$$

in which K_I is the stress intensity factor and $\varphi(\theta)$ gives the spatial variation in the stress field around the crack tip. This expression recovers the $r^{-1/2}$ singular behavior for a smooth crack when $D = 1$. The primary effect of this altered geometric description is to lower the strength of the stress singularity. While attempting to account for the fine structure of fracture geometry, these approaches neglect any refinement in modeling the physics of fracture mechanisms. In addition, the application of mathematical fractals with infinite levels of feature generation leads to non-physical difficulties such as the lack of rectifiability of line segments because all segments theoretically have an infinite extent and the impossibility of defining surface normals due to the non-differentiability of the fractal curve. In the present research, the use of infinitely descending fractals is avoided because the fractal nature of fracture in solids is physically bounded, and the smallest scale cannot be less than the interatomic spacing of atoms in a crystal or amorphous solid. Although useful in the framework of classical fracture mechanics, stress singularities have no physical meaning at atomic length scales. The minimum fractal feature characteristics place a limit on the extent of generation of fine structure in fractal constructs. This limits the geometric complexity along any segment of a fractal curve and permits a statistical approach to be used in defining surface normal vectors.

Three different independent quantities are needed to define the energetics of fracture. One quantity is the energy of fracture formation that depends on the type of surface that is formed, whether it is a grain boundary surface or a surface inside a gain. This is important because each type of fracture surface consumes different energy per unit of surface area created. For intergranular fracture, the energy is dependent on the strength of the boundary between two grains which can be associated with the number of coincident lattice sites occupied. The next important factor to include is a statistical description of the crack surface characteristics such as relative orientation to external applied loads. Finally, the geometrical aspects of fracture surfaces need to be accurately accounted for, which involve the fractal character of fracture processes.

2.6 Energetics of Fracture

In order to estimate the energy required to separate a surface along a grain boundary or slip plane, we need to express the total binding energy as an integral along the surface to be separated. Such a surface will have certain grain or crystallographic parameters that

describe it. For example, these nanostructural parameters include grain orientation, mismatch angle and order of coincident lattice sites when dealing with an intergranular crack, and the orientation and initiation of crystal slip systems when dealing with transgranular fracture surfaces, etc. The values of these parameters may be defined as a function of the normal to the surface of the crack. The orientation of the surface normal is denoted by the variable ξ, and the separation energy density for the various parameters is given by the function $g(\xi)$. Let A be the total fracture surface to be created during some spatial increment using a local area coordinate, a, along the fractal surface. The orientation of the normal is, in turn, a function of the area coordinate such that $\xi = \xi(a)$. We can then write the separation energy U for generating a unit area of fracture surface as the integral

$$U = \frac{1}{A}\int g\left[\xi(a)\right]da \tag{7}$$

Classical fracture mechanics assumes that the surface is smooth and integration can then be defined by Riemann sums. Real cracks, however, are rough, and a reexamination of the concept of an integral for such surfaces is needed. In doing so, the normal at each segment of a rough surface and the individual area elements must be defined, and the overall integration process must be formulated.

As a theoretical starting point, it is assumed that the rough surface can be described by infinitesimal area elements and that a normal to the differential surface can be defined. Consider the examples presented in Figure 8. In the case of a flat (classical) fracture surface, a single unit vector describes the normal to the surface and energy quantities can be integrated over the domain using classical limits. In the segmented curve case of Figure 8, there are three different slopes with three normal orientations that can be assumed to exist over the same area element. To treat this multiplicity mathematically, it is assumed that each normal appears with a certain probability. The way to describe it is in terms of a probability density function $f(\xi)$. For the segmented curve, we can express the probability of normal orientation as

$$f(\xi) = \alpha_1\delta(\xi - \xi_1) + \alpha_2\delta(\xi - \xi_2) + \alpha_3\delta(\xi - \xi_3) \tag{8}$$

where δ is the Dirac delta function and α_i are the relative frequencies of each normal orientation. The last case in Figure 8 shows a fractal-like surface where, for a mathematical fractal, the normal attains infinitely many values at each point and the probability density function becomes continuous.

In mathematical language, the surface normals of typical cracks are not uniquely defined vectors associated with classical smooth functions, but may instead be described by formal measures [20]. For practical applications, these measures can be approximated while preserving the degree of accuracy in the overall integration of surface energetics. An intuitive understanding of the measures used here is provided by the use of probability distribution functions.

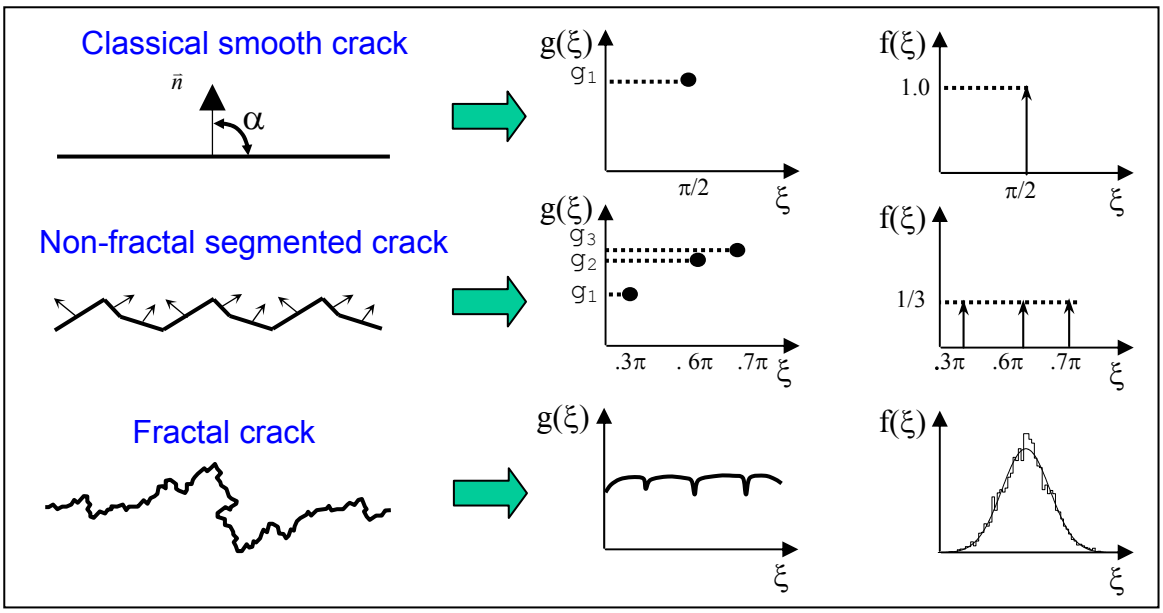

Figure 8. Fracture profiles with associated energy measures as a function of surface normal orientation and probability density functions.

2.7 Integration on rough surfaces

Assuming a crack path with a uniform extension in the thickness coordinate, the definition of an area element, Δa, is based on an extension of Equation (3) yielding a relationship given by

$$\Delta a = \varepsilon (\delta a / \varepsilon)^{D} \tag{9}$$

where Δa is the area of an oriented small surface element along the fractal curve, δa is the reflection of the oriented surface onto a flat plane, and ε is the smallest characteristic feature length of the fracture surface. This formula scales the classical area element, Δa, to reflect the fact that the surface is not smooth but contains several scales of smaller features that cannot be neglected, as they contribute to a different effective area. For integration purposes, Equation (9) can be generalized to yield a formula for the area element that includes any number of scales, with different fractal characteristics, each spanning its own dimensional range.

To integrate an energy density function as an infinitesimal quantity defined continuously along a rough surface, we need to know the relative occurrence in the form of a probability density function of the different values of the nanostructural parameter at each point. The probability density function $f(\xi)$ associated with a particular parameter is used such that $f(\xi)d\xi$ is the probability of having a nanostructure parameter in the range $(\xi, \xi + d\xi)$. This quantity depends only on the surface geometry such as orientation,

mismatch angle, etc. Because the function $g(\xi)$ is multivalued at each point in the domain, the function value in the limit as $\Delta a \rightarrow da$ is indefinite and the Riemann integral over the surface is not defined. Therefore, the way to integrate $g(\xi)\, da$ is to perform an additional integration over the parameter space using the probability density function $f(\xi)$. A formal measure of the value of the integrand at each point is obtained by integrating over all possible values of the energy function with its associated probability. The resulting correspondence in terms of measurement of energy density over a differential area element is given by

$$g[\xi(a)]da \Leftrightarrow da\int g(\xi)f(\xi)d\xi \tag{10}$$

In the application to real fracture surfaces with bounded fine-structure, the assumption of infinitesimal features is no longer valid. This bound on computed quantities leads naturally to an approximation by sums. Therefore, Equation (10) is modified by assuming a piecewise constancy of a particular value of the structural parameter, ξ_j, each of which is associated with a small element area domain, Δa_j, and replacing the integral with a sum over the entire area domain A where the index j is associated with each individual area domain.

Another necessary modification of the integration scheme involves applying the concept of measurement by condensing the sums of $g(\xi_j)$ and Δa_i over all values of the index j into reduced sums over the number of unique values of the structural parameter indexed by the variable η. This yields an effective representative surface in which each condensed area element is associated with a relative frequency of multiple values for the energy density function. For example, the simplified density function given by Equation (8) referring to the segmented crack depicted in Figure 8, gives $\eta = \{0.3\pi, 0.6\pi, 0.9\pi\}$. Utilizing summation by parts we can derive a reduced sum over η for the energy density as

$$\int_A g[\xi(a)]da = \sum_j g(\xi_j)\Delta a_j = \sum_\eta \sum_{j:\xi_j=\eta} g(\eta)\Delta a_j = \sum_\eta g(\eta) \sum_{j:\xi_j=\eta} \Delta a_j = \sum_\eta g(\eta)\Delta a(\eta) \tag{11}$$

where $\Delta a(\eta)$ is the sum of all area elements, Δa_j, that correspond to a given value of the energy function, i.e. $g(\xi_j) = g(\eta)$. The final sum in Equation (11) can then be expanded to introduce the relative frequency of $\Delta a(\eta)$ as

$$\sum_\eta g(\eta)\Delta a(\eta) = \sum_\eta g(\eta)\left(\frac{\Delta a}{\sum_\eta \Delta a(\eta)}\right)\Delta a(\eta) = \sum_\eta g(\eta)f(\eta)\Delta a \tag{12}$$

The resulting sum over all η partial sums yields the total area given by

$$A = \sum_\eta \Delta a(\eta) \tag{13}$$

and the probability density function $f(\eta)$ for the η^{th} value of the energy density is given by

$$f(\eta) = \frac{\Delta a(\eta)}{\sum_{\eta} \Delta a(\eta)} \tag{14}$$

This ratio represents the relative occurrences of Δa_η for which the nanostructural parameter ξ_η attains a distinct value with respect to the local area, Δa. Thus, we may now write the final relationship between the integrated value of the function $g(\xi)$ over the physical domain, A, in terms of discretized measures as

$$\int_A g[\xi(a)]da = A \sum_{\eta} g(\eta) f(\eta) \tag{15}$$

This yields a constructive way for obtaining the relative frequency of the value $g(\eta)$ given in Equation (15). Thus, the integral of the energy density function with multivalued functions expressed in terms of probabilities is a directly computable quantity, obtained by a simple consideration of the surface geometry.

2.8 Strain Energy Release Rate

The application of these ideas can now be used to define a strain energy release rate. In the hierarchical model developed here, information must be combined across several dimensional scales. At the nanoscale, the complete material energetics defined by several nanostructural variables may be characterized by a multivariate separation energy density function, $g[\chi_\iota(\xi)]$, obtained from atomistic simulation. At mesoscale dimensions, the crack surface characterization may be described by a density function of relevant values of nanostrutural parameters, $f[\chi_\iota(\xi)]$. The density function is obtained from a mesoscopic percolation model in which a sequence of random grain structures and crack propagation is repeatedly analyzed to accumulate the statistics of crack profiles causing material separation. The progression of a particular 'realized' crack through the material domain causing complete separation of the model is referred to as crack percolation. Performing meso-to-macroscale transformation of crack energy is accomplished by scaling using the fractal dimension that persists over several orders of magnitude. This scaling is expressed by an area definition given by

$$\int_A da = A_o^D \, \varepsilon^{1-D} \tag{16}$$

where A_o is the projection of the total fracture surface onto a flat plane.

Putting all these together, the standard definition of strain energy release for a solid based on surface energy γ_s [4] and plastic deformation energy γ_p [21] given by

$$G_c = \left.\frac{\partial U}{\partial A}\right|_c = 2\gamma_s + \gamma_p \tag{17}$$

can be replaced with a definition that accounts for the fractal nature of the surface and atomistic mechanisms of energy consumption along the surface given by

$$G = \langle g \rangle = \frac{\int_A g[\xi(a)]da}{\int_A da} = A_o^{-D}\,\varepsilon^{D-1}\int g(\xi)f(\xi)d\xi = A_o^{-D}\,\varepsilon^{D-1}\sum_{i=1}^{N} g(\xi_i)f(\xi_i) \tag{18}$$

where N is the number of unique values in the discrete spectrum of the nanostructural parameters. Equation (18) constitutes a replacement of the empirical definition of classical strain energy release by relating the probability density of nanoscale unit energy measures of fracture surface creation obtained by atomistic simulation to macroscopic length scales. This relationship is rigorously quantified by the use of the fractal dimension which constitutes a magnification factor that yields a true measure of created fracture surface areas. The present formulation is focused on brittle fracture in which γ_s is the predominant contributor to crack energetics. The treatment of dislocation mechanisms and associated energy dissipation contributing to the plastic work, γ_p, which predominate in the fracture of ductile materials remains a topic of future work.

3.0 Practical Implementation

A computational framework is introduced for incorporating the results of atomistic simulations into a mesoscopic percolation model of fracture in polycrystalline metals from which macroscopic fracture parameters can be predicted.

The theoretical approach presented in Sections 2.0 to 2.8 for estimating strain energy release rate incorporates several physical and geometric quantities. Specifically, information is needed regarding separation energies, $g(\xi)$, fracture characterization, $f(\xi)$, and fractal dimension, D. To find a relation between $g(\xi)$, $f(\xi)$, and D, a mesoscopic simulation procedure is developed using a percolation model of crack formation and propagation.

3.1 A Computational Framework

In order to achieve a realistic estimate of macroscopic fracture parameters of interest, failure phenomena must be modeled over several dimensional scales. Atomistic simulation can give realistic approximations of intergranular and transgranular separation energies at the nanoscale. These simulations need to be performed for the full spectrum of grain orientations, boundary mismatch angles, etc. such that the parameter space is fully sampled. At the grain level, the energy of grain boundary separation and dislocation evolution must be calculated as a result of mechanical and thermal stresses. At the mesoscale level, a large network of grains needs to be modeled in order to simulate the

formation of complex crack structures. The result of these Monte Carlo-type simulations can then be applied to develop statistics of fracture formation and propagation.

3.2 Atomistic Simulation of Fracture

Nanoscale simulation of fracture phenomena is performed using molecular dynamic methods for calculating atomic trajectories and interaction energies [22,23]. Basic phenomena of intragranular dislocation formation and progression, and separation along

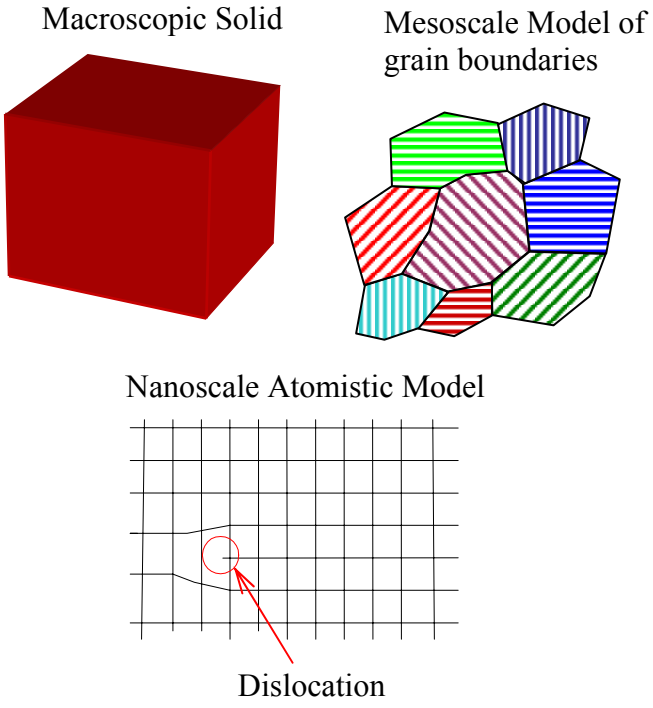

Figure 9. Computational regimes.

grain boundaries can be simulated such that the relevant physical quantities of separation energy can be determined. These quantities are calculated for a range of parametric values that are then integrated using appropriate probabilistic distributions to obtain a statistical summation such as given by Equation (18). These simulations provide predictions of grain boundary strength based on relative angular orientation of adjacent grains and the energy consumed in the coalescence of voids in an idealized grain field. Typical atomistic simulations of grain boundary separation and the growth of a simulated void in an isotropic solid under applied loads are shown in Figures 10 and 11, respectively. Figure 10 shows the prediction of peak separation stress and energy of two grains of aluminum subjected to a normal applied opening displacement. The two grains have crystallographic orientations given by the Miller indices [100] and [310] which dictate the strength of the boundary region in the bicrystal. This simulation is an example of the parametric analyses that need to be performed to ascertain the boundary strength

between grains of different relative orientation. These types of simulations can be used to predict the energetics of brittle intergranular fracture.

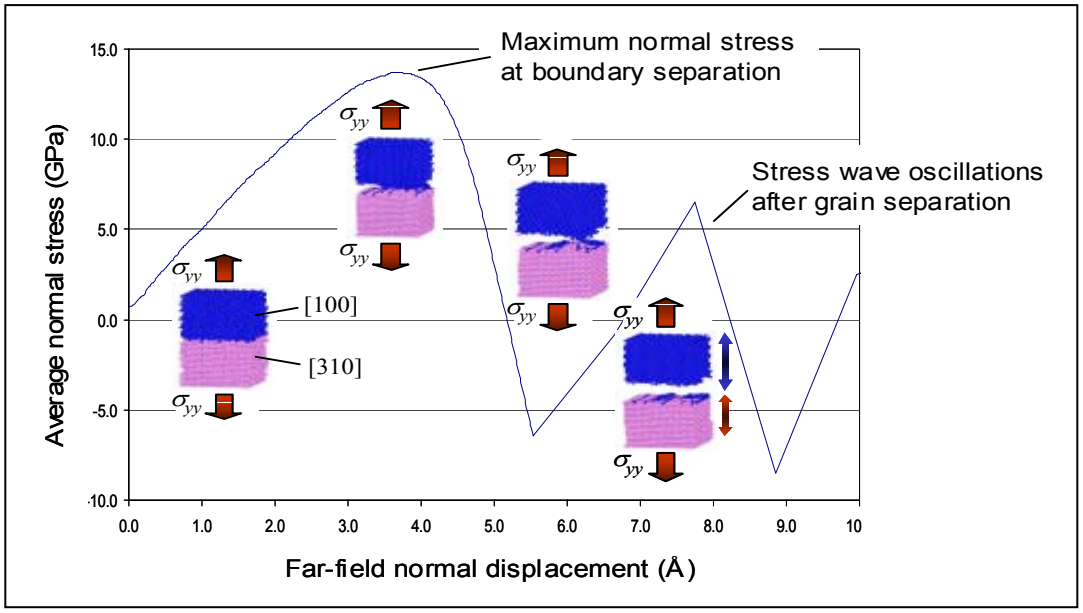

Figure 10: Atomistic simulation of separation between [100] and [310] planes of Al.

Figure 11 shows the atomistic simulation of a void in an idealized microstructure being extended by applied displacements. The model consists of hexagonal grains of aluminum with missing grains representing the void. This model yields predictions of both the separation energy involving both intergranular and transgranular separation together with predictions of plastic deformation within grains. Because MD analysis records the behavior of every atom in the simulations, energy and deformation can be separated into elastic and plastic components for any group of atoms. An effective total energy of local defect propagation can also be calculated and used depending on the resolution of the continuum mesoscale model.

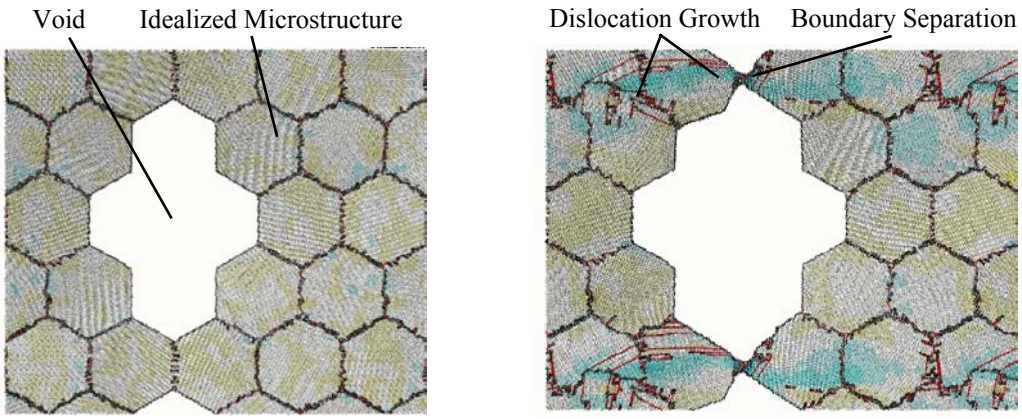

Figure 11. Atomistic simulation of deformation and separation of a void in an idealized microstructure.

The parametrically calculated energies of fracture formation obtained from nanoscopic models of atomistic mechanisms are used as input to a mesoscale model of fracture development. Computing crack propagation due to intergranular and transgranular fracture constitutes a general percolation sequence and, for that reason, the mesoscale representation is labeled a Percolation Model. The inputs to this model are grain structure, grain boundary strengths, and intergranular separation energy used to efficiently simulate a multitude of simulated fracture profiles for statistical interpretation. In the current study, mechanisms associated with plasticity are neglected.

3.3 A Percolation Model of Crack Coalescence

Percolation theory is one of the simplest models of a system containing random disorder [24]. Applied to the lowest-level continuum scale, percolation provides a framework that captures realistic crack formation, exhibiting correct material-specific deformation processes and geometric properties. The result of this analysis is to predict the coalescence of defects and local failures leading to the progression of dominant cracks.

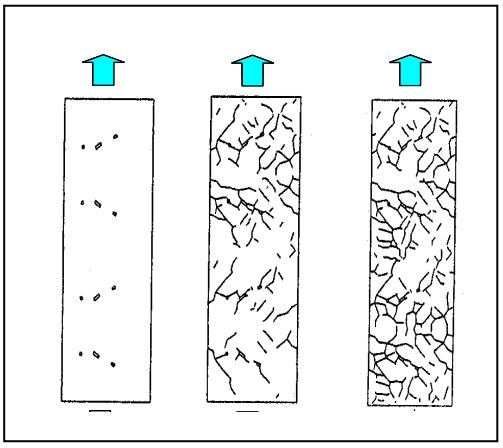

Figure 12. Coalescence of microcracks.

In fracture processes, percolation is strictly associated with growth and coalescence of voids. If the interaction of voids were neglected, the resulting fractal dimension would be universal or invariant, which is generally not true. In the present analysis, initial voids and other defects are influenced by neighbors and do not yield a universal fractal dimension to describe coalescence behavior. The predicted percolation sequence of initial defects gives rise to the particular fractal characteristics of crack geometry.

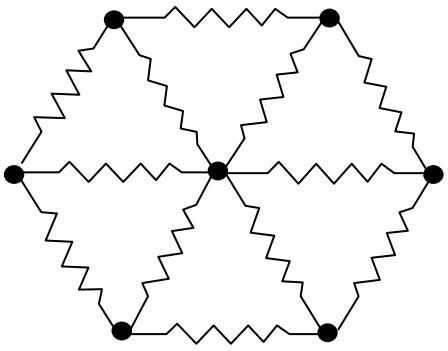

Figure 13. Unit hexagonal spring network.

A finite element discretization of the domain is performed using hexagonal spring units as shown in Figure 13. The use of a spring model was selected as a proof-of-concept simplification to model an isotropic continuous medium containing weak boundaries. These boundaries correspond to the region of adjoining grains and can potentially separate to form local cracks. Crack surfaces in this model are defined orthogonal to the springs. Since metals are polycrystalline in most application, the granular structure is incorporated into the model. Grain stiffnesses and grain boundary strengths determined through the

atomistic simulations are input as effective spring properties. This simplified mesoscalae model is the first step towards a more computationally intense finite element representation using two- three-dimensional continuum element formulations and cohesive zone elements to model mixed-mode separation along boundaries [25].

Simulations begin by establishing a realistic grain structure. This structure is obtained from a Monte Carlo simulation that incorporates grain boundary physics such as the Mullins equation of curvature driven growth, enforcement of the Herring condition at triple junctions, and von Neumann conditions for grain stability [26]. A sample of such grain configuration is shown in Figure 14. A uniform network of springs having hexagonal connectivity is projected onto the network of grains. Springs that cross a grain boundary are assigned spring constants representing the effective stiffness of the boundary. The spring model, therefore, does not represent individual atomistic interactions, but simulates an anisotropic mesoscale continuum based on aggregate atomic behavior.

Initial flaws in the material are introduced at random positions according to a prescribed ratio. These flaws are represented in the model as broken springs, i.e., their spring constants are set to zero. The flaws may correspond to voids, pores, and nanoscale cracks, that may exist at both intergranular or transgranular sites. The diagram in Figure 15 shows a sample configuration with defects modeled by selectively deleting the corresponding springs.

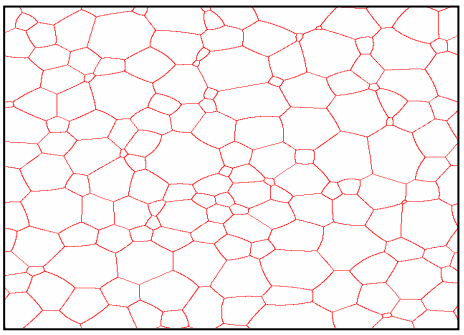

Figure 14. Simulated grain structure.

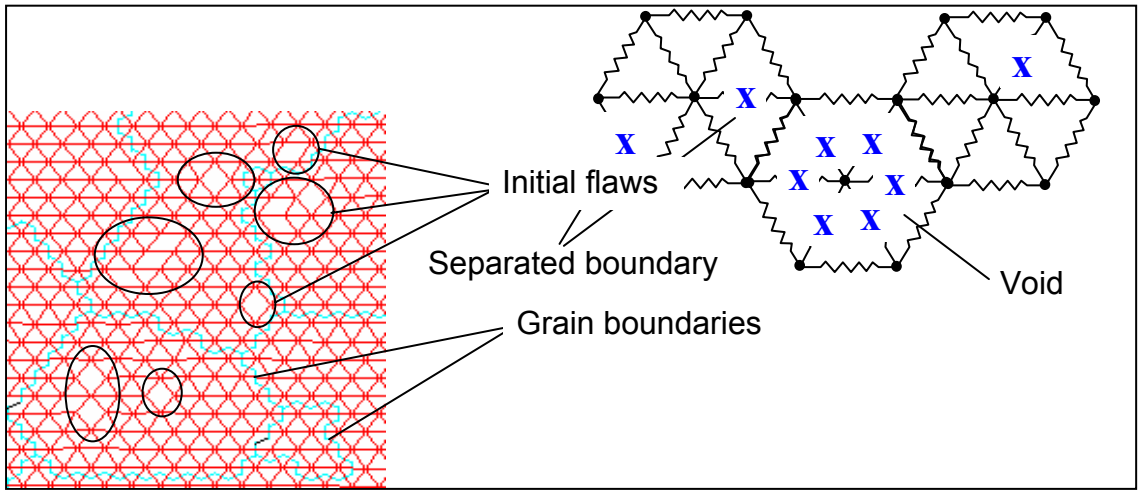

Figure 15. Representation of imperfections in percolation model.

3.4 Illustrative Mesoscale Simulation Results

A hexagonal spring model shown in Figure 16 is used to simulate percolation due to the formation and development of cracks for a wide range of parameters in terms of initial defects, spring strengths, etc. A two-dimensional model is chosen with randomly distributed defects. The initial amount of damage (voids and separated boundaries) modeled by degraded springs was fixed at two percent of the total number of springs used to model the continuum. The model is clamped at one end and loaded by enforced displacements at the other end. Figures 17 through 21 show snapshots of simulations in which different distributions of initial defects are present.

The simulations are shown to predict single and multiple dominant crack formation and progression, island formation, and branching patterns. The fractal-like quality of the fracture surface is clearly captured in these simulations. The simulations are performed on domains with the same size and with the same percentage of defects. The figures show successive images just before and after final fracture.

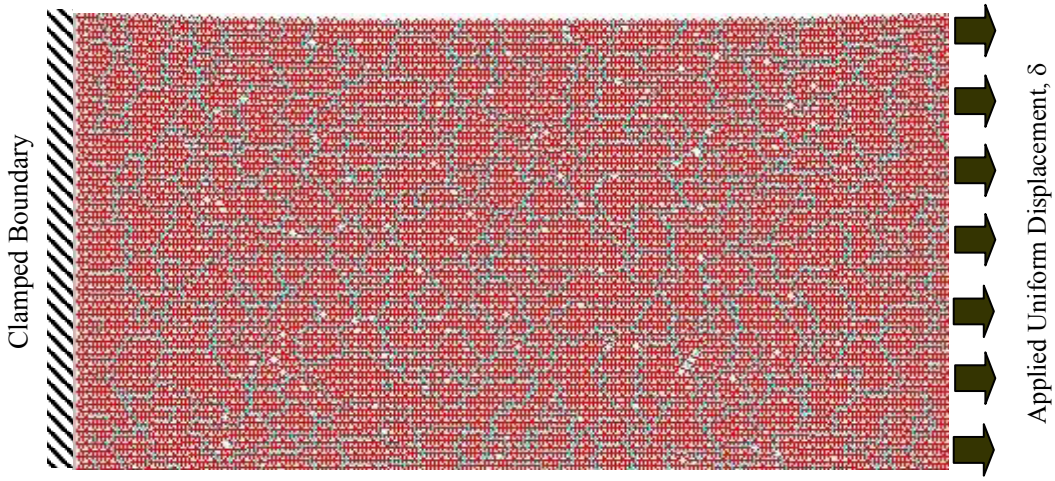

Figure 16. Initial model depicting grain structure and random imperfections

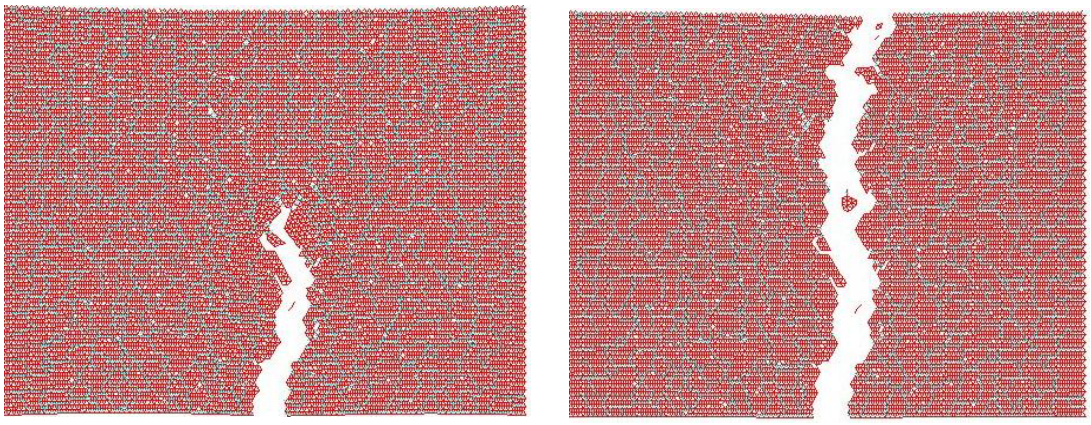

Figure 17. Test no. 1: Frames 5 and 6.

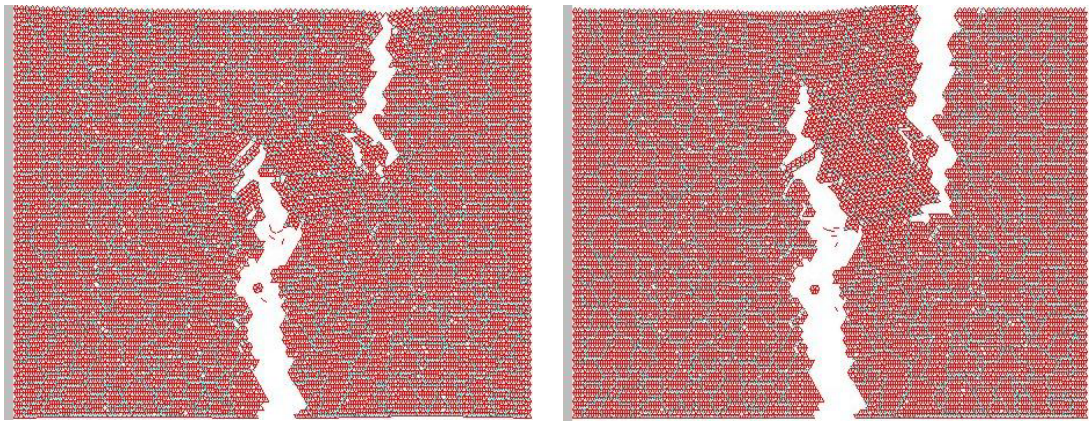

Figure 18. Test no. 2: Frames 12 and 13.

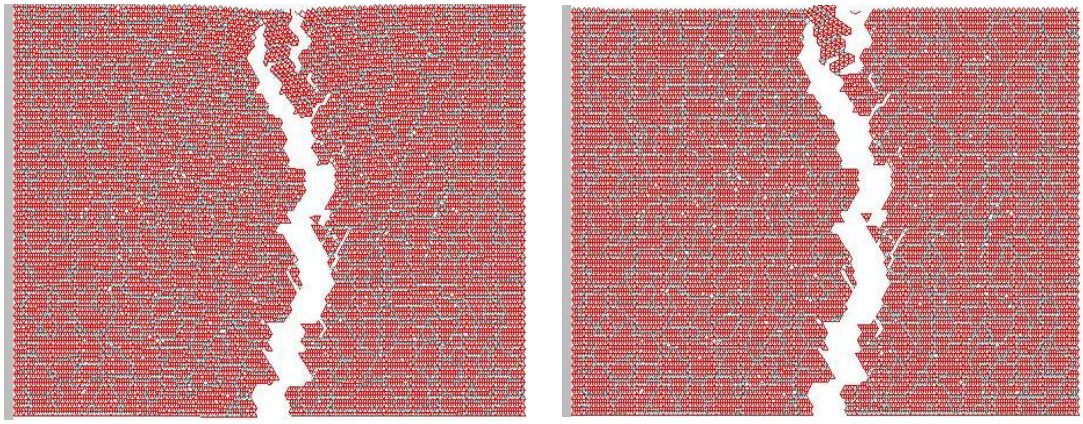

Figure 19. Test no. 3: Frames 11 and 12.

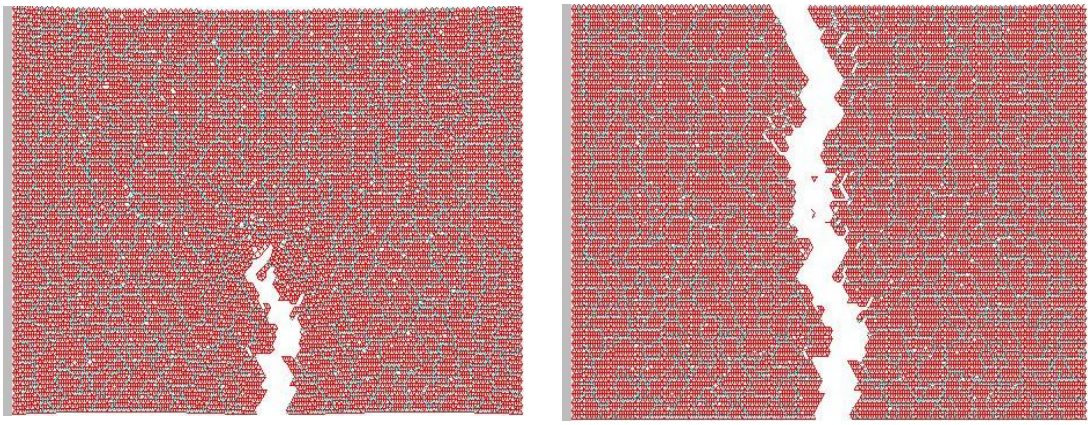

Figure 20. Test no. 4: Frames 5 and 7.

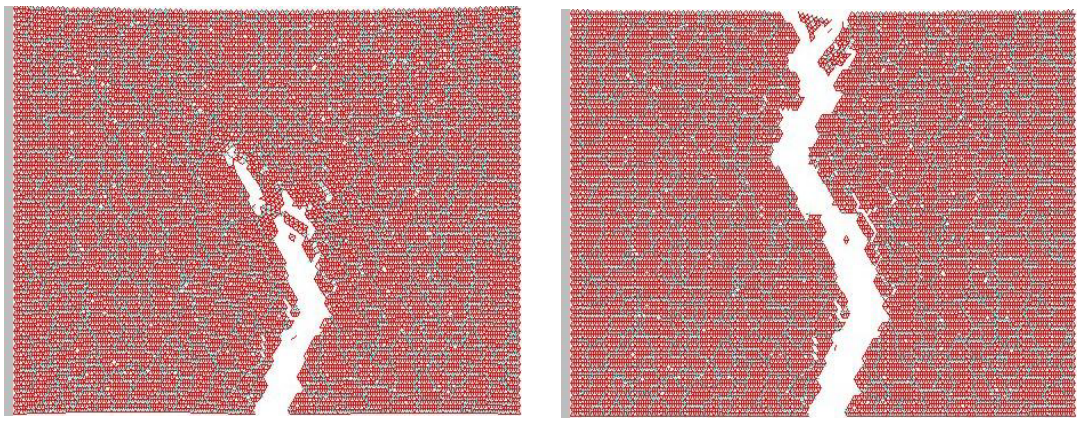

Figure 21. Test no. 5: Frames 6 and 7.

All numerical tests were run using the same applied displacements and fixity boundary conditions. The models fractured at different elongation magnitudes showing that the variability in the fracture toughness due to random initial microcracks is large. This variability demonstrates the need for statistical interpretation of results which is unavailable from idealized classical models of fracture. This analysis constitutes a Monte Carlo simulation using the mesoscale model. The accumulated results yield the fractal dimensions of the fracture geometry together with the statistics required to integrate the underlying energy measures of crack formation. The energetics of fracture at the mesoscale are then scaled using the Hausdorff dimension of the assumed underlying fractal geometry to yield macroscopic estimates of strain energy release by applying Equation (18), derived in Section 2.8.

4.0 Concluding Remarks

An initial framework for a hierarchical fracture mechanics has been developed. The hierarchical model encompassing atomistic simulation, polycrystal fracture nucleation and growth, and fractal geometry characterization has been shown to be a viable approach for predicting strain energy release rates from first principles. Simulations need to account for flaw types and failure processes at the atomistic level to fully describe the mechanisms of fracture. Surface separation and plastic deformation energies can be obtained using current atomistic simulation methods. Interaction of damage growth mechanisms will require models with large atomic ensembles but mitigate the empiricism of experimentally determined fracture parameters. Mechanisms involving plasticity present an additional degree of complexity and need to be fully incorporated into the analysis through extension of the mesoscale percolation model. Finally, for a basic validation of the hierarchical analysis, predicted crack path characteristics, fracture surface geometry, and predicted values for fracture parameters need to be correlated with experimental results.

5.0 References

1. Hutchinson, J.W. and Evans, A.G., "Mechanics of Materials: Top-Down Approaches to Fracture," *Acta. Mater.* ,**48**, pp. 125-135, 2000.
2. Hafner, J., "Atomic-Scale Computational Materials Science," *Acta. Mater.*, **48**, pp.71-92, 2000.
3. Needleman, A., "Computational Mechanics at the Mesoscale," *Acta. Mater.*, **48**, pp.105-124, 2000.
4. Griffith, A.A., "The Phenomenon of Rupture and Flow in Solids," *Philos. Trans. R. Soc. London, Ser. A*, **A221**, pp. 163-198, 1924.
5. Fleck, N.A. and Hutchinson, J.W., "Strain Gradient Plasticity," *Adv. Appl. Mech.*, **33**, pp. 295-361, 1997.
6. Mandelbrot, B.B. *The Fractal Geometry of Nature*, New York: W.H. Freeman, 1982.
7. Schroeder, M., *Fractals, Chaos, Power Laws*, New York, W.H. Freeman, 1999.
8. Barnsley, M.F., *Fractals Everywhere*, Mogan Kaufmann, 1993.
9. Mandelbrot, B.B., "Self-Affine Fractals and Fractal Dimension," *Physical Scripta*, **32**, pp. 257-260, 1985.
10. Mandelbrot, B.B., Passoja, D.E., and Paullay, A.J., "Fractal Character of Fracture Surfaces of Metals," *Nature*, **308**, pp. 721-722, 1984.
11. Passoja, D.E., and Amborski, D.J., "Fracture Profile Analysis by Fourier Transform Methods," *Microstruct. Sci.,* **6,** pp.143-148, 1978.
12. Charkaluk, E., Bigerelle, M., and Iost, A., "Fractals and Fracture," *Eng. Fract. Mech.*, **61**, pp. 119-139, 1998.
13. Dougan, L.T., Addison, P.S., and McKenzie, W.M.C., "Fractal Analysis of Fracture: A Comparison of Dimension Estimates," *Mech. Res. Commun.*, **27**, pp. 383-392, 2000.
14. Hornbogen, E., "Fractals in Microstructure of Metals," *Int. Mat. Rev.*, **34**, pp.277-296, 1989.
15. Carpinteri, A., Chiaia, B., and Cornetti, P., "A Scale-Invariant Cohesive Crack Model for Quasi-Brittle Materials," *Eng. Fract. Mech.*, **69**, pp. 207-217, 2002.
16. Ta'asan, S. "Mathematics of Fractals," NASA Final Report, PO No. L-17941, Carnegie Mellon University, Oct. 2003.
17. Yavari, A., Hockett, K.G., and Sarkani, S., "The Fourth Mode of Fracture in Fractal Fracture Mechanics," *Int. J. of Fract.*, **101**, pp. 365-384, 2000.
18. Yavari, A., Sarkani, S., and Moyer, E.T., "The Mechanics of Self-Similar and Self-Affine Fractal Cracks," *Int. J. of Fract.*, **114**, pp. 1 - 27, 2002.
19. Cherepanov, G.P., Balankin, A.S., and Ivanova, V.S., "Fractal Fracture Mechanics – A Review," *Eng. Fract. Mech.*, **51**, pp. 997-1033, 1995.
20. Allen, M.J. and Yen, W.M., *Introduction to Measurement Theory*, Waveland Pr Inc., 2001.
21. Orowan, E., "Fracture and Strength in Solids," *Reports on Progress in Physics,* **XII**, p. 185, 1948.
22. Allen, M.P., and Tildesley, D.J, *Computer Simulation of Liquids*, Clarendon Press, Oxford, 1987.
23. Haile, J.M., *Molecular Dynamics Simulation, Elementary Methods*, John Wiley & Sons, Inc. 1991.
24. Stauffer, D. and Aharony, A., *Introduction to Percolation Theory*, 2nd. ed. (Taylor and Francis, London, 1992).
25. Jin, Z.H., Paulino, G.H., and Dodds, R.H., Jr. "Finite Element Investigation of Quasi-Static Crack Growth in Functionally Graded Materials Using a Novel Cohesive Zone Fracture Model," *J. Appl'd Mech.*, **69**, pp. 370-379, 2002.
26. Anderson, M.P., Srolovitz D.J. et al, "Computer Simulation of Grain Growth I. Kinetics," *Acta Metallurgica*, **32**, pp. 783-791, 1985.

REPORT DOCUMENTATION PAGE

Form Approved
OMB No. 0704-0188

1. REPORT DATE *(DD-MM-YYYY)*	2. REPORT TYPE	3. DATES COVERED *(From - To)*
01- 11 - 2004	Technical Memorandum	

4. TITLE AND SUBTITLE
A Hierarchical Approach to Fracture Mechanics

5a. CONTRACT NUMBER

5b. GRANT NUMBER

5c. PROGRAM ELEMENT NUMBER

6. AUTHOR(S)
Saether, Erik; and Ta'asan, Shlomo

5d. PROJECT NUMBER

5e. TASK NUMBER

5f. WORK UNIT NUMBER
23-762-55-LC

7. PERFORMING ORGANIZATION NAME(S) AND ADDRESS(ES)
NASA Langley Research Center
Hampton, VA 23681-2199

8. PERFORMING ORGANIZATION REPORT NUMBER
L-19061

9. SPONSORING/MONITORING AGENCY NAME(S) AND ADDRESS(ES)
National Aeronautics and Space Administration
Washington, DC 20546-0001

10. SPONSOR/MONITOR'S ACRONYM(S)
NASA

11. SPONSOR/MONITOR'S REPORT NUMBER(S)
NASA/TM-2004-213499

12. DISTRIBUTION/AVAILABILITY STATEMENT
Unclassified - Unlimited
Subject Category 39
Availability: NASA CASI (301) 621-0390

13. SUPPLEMENTARY NOTES
Saether: Langley Research Center; Ta'asan: Canegie Mellon University.
An electronic version can be found at http://techreports.larc.nasa.gov/ltrs/ or http://ntrs.nasa.gov

14. ABSTRACT

Recent research conducted under NASA LaRC's Creativity and Innovation Program has led to the development of an initial approach for a hierarchical fracture mechanics. This methodology unites failure mechanisms occurring at different length scales and provides a framework for a physics-based theory of fracture. At the nanoscale, parametric molecular dynamic simulations are used to compute the energy associated with atomic level failure mechanisms. This information is used in a mesoscale percolation model of defect coalescence to obtain statistics of fracture paths and energies through Monte Carlo simulations. The mathematical structure of predicted crack paths is described using concepts of fractal geometry. The non-integer fractal dimension relates geometric and energy measures between meso- and macroscales. For illustration, a fractal-based continuum strain energy release rate is derived for inter- and transgranular fracture in polycrystalline metals.

15. SUBJECT TERMS
Fracture mechanics; Strain energy release rate; Fractal geometry

16. SECURITY CLASSIFICATION OF:			17. LIMITATION OF ABSTRACT	18. NUMBER OF PAGES	19a. NAME OF RESPONSIBLE PERSON
a. REPORT	b. ABSTRACT	c. THIS PAGE			STI Help Desk (email: help@sti.nasa.gov)
					19b. TELEPHONE NUMBER *(Include area code)*
U	U	U	UU	29	(301) 621-0390